

# Performance Analysis of IPTV Traffic in Home Networks

Emad Shihab, Fengdan Wan, Lin Cai and Aaron Gulliver  
Department of Electrical and Computer Engineering  
University of Victoria, Victoria  
British Columbia V8W 2Y2, Canada

Noel Tin  
Broadband Home Technology Development  
Bell Canada, Toronto  
Ontario M5J 1A7, Canada

**Abstract**—A heterogeneous wired and wireless network architecture is proposed for in-home IPTV distribution. To identify the bottleneck in the home network and estimate the network capacity, we develop an analytical framework to quantify the maximum number of IPTV connections that can be supported with guaranteed QoS in the wired and multi-hop wireless networks, respectively. We extend the fluid flow model analysis to capture both the burstiness of IPTV sources and the time-varying characteristics of multi-hop wireless channels. Extensive NS-2 simulations with H.264 HDTV sources over wired and multi-hop wireless paths are given, which validate the analysis. The analytical and simulation results provide important guidelines for the planning of future home networks and IPTV systems.

**Index Terms**—home networks, IPTV, fluid model

## I. INTRODUCTION

Internet Protocol TV (IPTV) has been predicted to be a major technology winner. Telecommunication service providers are racing to deliver IPTV/video on demand (VoD), voice, and data, so called triple-play services. One of the major challenges in rolling out IPTV services is the design and development of the last-meter broadband home networks, such that consumers can enjoy TV and video anytime, in any room, *without rewiring* their houses. Competing wireless and wired communication technologies are emerging, e.g., Ethernet, MoCA, HPNA over phonelines or coax cables, HomePlugAV over powerlines or coax cables, IEEE 802.11n, UltraWide Band (UWB), millimeter-wave (mmWave), and will quickly reshape our vision of future home networks.

Because of the complimentary characteristics and disparities of wired and wireless communication technologies, the architecture of future broadband home networks are anticipated to be heterogeneous wireless and wired networks. Existing wired links will construct the backbone of home networks, which provide reliable, high data rate communications with QoS guarantees. Emerging high data rate wireless technologies will further deliver IPTV traffic to the whole home ubiquitously, through single-hop or multiple-hop paths. Given the architecture of hybrid networks and the throughput of both wired and wireless links, an immediate question is how many IPTV connections can be supported simultaneously with guaranteed QoS, or what is the admission region of IPTV traffic in a home network?

To answer this question, the quantitative analysis of how many IPTV connections can be supported in a home network is a key issue. This not only helps service providers and

consumers to choose the best technologies for home networking, but also provides important guidelines for planning the entire IPTV system. The main difficulties in quantifying the admission region are twofold. First, new video compression technologies, e.g, MPEG-4 H.264, for IPTV/VoD can achieve higher compression rates, but also bring higher burstiness (peak to average ratio) of the traffic. Second, wireless channels are time-varying, location dependent, and most wireless communication technologies adapt the data rate accordingly. The achievable flow throughput over a multi-hop wireless path is even more dynamic. To the best of our knowledge, no existing results quantify the admission region of highly bursty IPTV traffic over highly dynamic multi-hop wireless networks. In this paper, we develop a fluid model based analytical framework to quantify the admission region of IPTV traffic in wireless and wired home networks, considering the time-varying characteristics of multi-hop wireless channels and the highly bursty nature of IPTV traffic.

The main contributions of this paper are three-fold. We first propose a wireless and wired network architecture for in-home IPTV distribution. Second, we develop an analytical framework for quantifying the admission region of home networks, which reveals the relationship among system and QoS parameters. In addition, extensive simulation using MPEG-4 video traces and the publicly available NS-2 network simulator has been conducted, and the results validate our analysis.

The remainder of the paper is organized as follows. We introduce the network architecture and system model in Section II. The fluid model analysis to quantify the admission region for hybrid wireless and wired networks is given in Section III, followed by simulation and numerical results in Section IV. Section V presents the concluding remarks.

## II. SYSTEM MODEL

To support IPTV services anytime, in any room, without rewiring existing houses, we propose a hybrid wireless and wired network architecture for in-home IPTV distribution, as shown in Fig. 1. Existing wired links, like coax cables, phonelines and powerlines, construct the backbone of home networks. A few wireless access points (APs) and devices further relay the IPTV traffic to any corner of the home via single- or multiple-hops, using high data rate wireless communication technologies, e.g., IEEE 802.11n, UWB, mmWave, etc.

The wired backbone network, e.g., MoCA, HPNA, or HomePlugAV over coax cables, can achieve high data rates

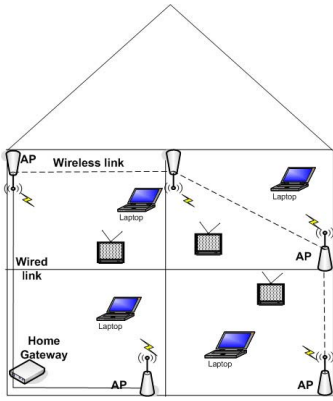


Fig. 1. Home network architecture

and high availability [2]. For instance, the measurement results for MoCA show that a throughput of at least 100 Mbps is achieved by 95% of the coax jacks tested. HPNA and HomePlugAV can also achieve similar performance. The MAC protocols specified in these competing standards can support TV/Video applications with QoS guarantees.

In the wireless domain, although different technologies use different MAC protocols, to support multimedia applications with stringent QoS requirements, the basic architecture and approach are similar. We adopt the architecture and MAC protocol specified in IEEE 802.15.3 in our system model.

IEEE 802.15.3 is the standard dedicated to wireless personal area networks (WPANs). Several devices can autonomously form a piconet in which one of them is selected as the piconet coordinator (PNC). The PNC can collect global information about the piconet and allocate radio resources or schedule channel times to all devices in the piconet according to their requests, and all devices can communicate in a peer-to-peer fashion using the allocated channel time. Such a semi-ad hoc setting can provide better QoS than a pure ad hoc network. In the standard, time is slotted into a superframe structure where each superframe consists of a beacon period (BP), a contention access period (CAP) using CSMA/CA as the access protocol, and a contention-free period named channel time allocation period (CTAP) using Time Division Multiple Access (TDMA). All devices can request channel time through contention in the CAP, and use the allocated channel time in the CTAP for transmission. If the traffic must be relayed with multiple hops, the PNC should allocate separate time slots for each hop.

Since the wireless channel condition is time-varying, most wideband wireless technologies adapt the data rate according to the channel condition. For instance, the over-the-air data rate of IEEE 802.11n varies from 200 Mbps to 540 Mbps, and that of UWB varies from 53.3 Mbps to 480 Mbps or even higher. With the physical layer rate adaptation and the link layer retransmissions, from the upper layer protocols' point of view, packet losses due to transmission errors are negligible. However, the link throughput (or data rate) observed by the upper layer protocols is time-varying. Since the wireless link throughput is time-varying and channel-condition dependent, the same packet over different hops may request different amounts of time due to their different data rates. We choose

the widely adopted finite state Markov model as the packet-level wireless channel model, because it is recognized to be reasonably accurate in capturing wireless channel variations. With this model, the wireless channel evolves as a finite state Markov chain, where each state corresponds to a different average Signal to Noise Ratio (SNR) and thus a different data rate. The state-transition probabilities are appropriately chosen to reflect the time-correlation of the wireless channel.

For IPTV video sources, advanced source coding technologies have been developed to aggressively increase the compression ratio and reduce the source data rate. Video frames (I, P and B) are compressed by canceling temporal and spatial redundancy. Since H.264/AVC (MPEG-4 Part 10) has about twice the compression efficiency compared to that of MPEG-2, it is anticipated to be widely deployed in the transmission and storage of high definition (HD) content. For this reason, we consider H.264/AVC video sources in our system.

### III. FLUID MODEL ANALYSIS

To quantify the number of IPTV connections being supported with satisfactory QoS and identify the bottleneck in the home, we consider three scenarios separately: IPTV traffic over a wired link with a constant data rate, a single-hop wireless link with a variable data rate, and a multi-hop wireless path.

#### A. Fluid model of video traffic with constant server rate

Inside the home, all IPTV downstream traffic is delivered from the home gateway to different set-top boxes or devices. All transmissions in the wired network are in the same collision domain, and thus share the wired link bandwidth which is assumed constant. For video transmissions over constant data rate links, the well known fluid model can be directly applied. In [3], a variable bit rate video source is modeled as the multiplexing of 20 mini sources. Each mini source independently alternates between an "off" state and an "on" state, and  $A$  bps are generated during the "on" state. The average residence time in the "off" state and "on" state are  $1/\alpha$  and  $1/\beta$ , respectively. Since H.264 is much more efficient than the source codes considered in [3], we use fewer mini sources to emulate the more bursty video sources. Our simulation results suggest that using 8 mini sources to model one video source is appropriate.

Let  $F_i(x)$  denote the probability that the queue length is less than  $x$ , given that  $i$  mini sources are on. With a constant service rate of  $C$  bps and  $M$  mini sources in total, the equilibrium queue length distribution at the home gateway is subject to [3]

$$\frac{d\mathbf{F}(x)}{dx} \mathbf{D} = \mathbf{F}(x) \mathbf{B}_s \quad (1)$$

where  $\mathbf{D}$  is an  $(M+1) \times (M+1)$  diagonal matrix

$$\mathbf{D} = \text{diag}\{-C, 1-C, \dots, MA-C\},$$

and  $\mathbf{F}(x)$  is the row vector  $[F_0(x) \ F_1(x) \ \dots \ F_N(x)]$ . The underlying continuous time Markov chain of the video source

model is represented by the generating matrix

$$\mathbf{B}_s = \begin{pmatrix} -M\alpha & M\alpha & 0 & \cdots \\ \beta & -(M-1)\alpha - \beta & (M-1)\alpha & \cdots \\ \vdots & \vdots & \vdots & \vdots \\ 0 & \cdots & \cdots & -M\beta \end{pmatrix}$$

Given the fluid model, we can obtain the cumulative distribution function (CDF) of the queue length distribution as [4]

$$F(x) = 1 + \sum_{i: \text{Re}[z_i < 0]} a_i \sum_{j=1}^M \phi_{ij} \exp(z_i x),$$

where  $z_i$  and  $\vec{\Phi}_i$  are the negative left eigenvalues and the corresponding eigenvectors of the matrix  $\mathbf{B}' = \mathbf{B}_s \mathbf{D}^{-1}$ :

$$z_i \vec{\Phi}_i \mathbf{D} = \vec{\Phi}_i \mathbf{B}_s.$$

The coefficients  $a_i$  can be obtained from the boundary conditions, i.e.,  $F_j(0) = 0$  for  $j > C/A$ .

The survivor function  $G(x)$ , which represents the probability of buffer overflow, is the complementary distribution of  $F(x)$

$$G(x) = 1 - F(x) = - \sum_{i: \text{Re}[z_i < 0]} a_i \sum_{j=1}^M \phi_{ij} \exp(z_i x) \quad (2)$$

Given the QoS requirements of IPTV traffic, including loss rates and delay bounds, we can limit the number of connections and choose an appropriate buffer size accordingly. For instance, given the delay budget in a home network, we can determine the maximum queue length and thus the buffer size. From (2), we can determine the maximum number of connections that can be supported with a guaranteed loss rate due to buffer overflow.

Next, we extend the fluid model to analyze video traffic over single-hop and multi-hop wireless networks in which the link data rates are time-varying.

### B. Single hop wireless

For the wireless link, we use a finite state Markov model to model its time-varying data rates, with different states corresponding to different link data rates. Let  $C_j$  denote the data rate (service rate of the wireless link), when the wireless link is in state  $j$  and assume that the total number of states of the wireless link is  $N$ . The generating matrix of the underlying continuous time Markov process  $\mathbf{B}_c$  is defined by

$$\mathbf{B}_c = \begin{pmatrix} \mu_{11} & \mu_{12} & \mu_{13} & \cdots \\ \mu_{21} & \mu_{22} & \mu_{23} & \cdots \\ \vdots & \vdots & \vdots & \vdots \\ \mu_{N1} & \mu_{N2} & \cdots & \mu_{NN} \end{pmatrix}$$

where  $\mu_{kj}$ ,  $1 \leq k, j \leq N$  is the state transition rate from state  $k$  to state  $j$  and  $\mu_{kk} = -\sum_{j=1, j \neq k}^N \mu_{kj}$ .

Let  $F_{i,j}(t, x)$ ,  $0 \leq i \leq M$ ,  $1 \leq j \leq N$ ,  $t \geq 0$ ,  $x \geq 0$ , be the probability that queue length at the wireless AP does not exceed  $x$  at time  $t$ , when the wireless link is in state  $j$ , and

$i$  mini sources are on. The probability of one source turning on or turning off during a small time interval  $\Delta t$  is  $\alpha \Delta t$  or  $\beta \Delta t$ , respectively. Then we have

$$\begin{aligned} & F_{i,j}(t + \Delta t, x) \\ &= \sum_{k=1}^N [N - (i-1)] \alpha \Delta t F_{i-1,k}(t, x) \mu_{kj} \Delta t \\ &+ \sum_{k=1}^N (i+1) \beta \Delta t F_{i+1,k}(t, x) \mu_{kj} \Delta t \\ &+ \sum_{k=1, k \neq j}^N \{1 - [(M-i)\alpha + i\beta] \Delta t\} F_{i,k}(t, x) \mu_{kj} \Delta t \\ &+ \{1 - [(M-i)\alpha + i\beta] \Delta t\} F_{i,j}(t, x - (iA - C_j) \Delta t) \\ &\quad (1 - \mu_{jj} \Delta t) \\ &+ O(\Delta t^2) \end{aligned}$$

We are interested in the equilibrium probabilities, which are obtained when  $\Delta t \rightarrow 0$  and  $\partial F_{i,j} / \partial t = 0$ .

$$\begin{aligned} (iA - C_j) \frac{dF_{i,j}(x)}{dx} &= \sum_{k=1}^N [N - (i-1)] \alpha \Delta t F_{i-1,k} \mu_{kj} \\ &+ \sum_{k=1}^N (i+1) \beta \Delta t F_{i+1,k} \mu_{kj} \\ &+ \sum_{k=1}^N [(M-i)\alpha + i\beta] F_{i,k} \mu_{kj} \quad (3) \end{aligned}$$

Let  $\mathbf{F}'$  be the matrix with each component  $F(i, j) = F_{i,j}$ . We build a new row vector  $\mathbf{F}$  by concatenating  $\mathbf{F}'$  row by row and denoting  $F_k$  as the  $k$ -th component of  $\mathbf{F}$ , where  $k = N(i-1) + j$  for  $1 \leq k \leq N(M+1)$ . In matrix notation, (3) can be written as

$$\frac{d\mathbf{F}}{dx} \mathbf{D} = \mathbf{F} \mathbf{B} \quad (4)$$

which has the same structure as that in (1), where [5]

$$\mathbf{B} = \mathbf{B}_s \otimes \mathbf{I}_N + \mathbf{I}_{M+1} \otimes \mathbf{B}_c. \quad (5)$$

Here,  $\otimes$  is the Kronecker product [6], and  $\mathbf{I}_N$  is an  $N \times N$  identity matrix. Thus,  $\mathbf{B}$  is a matrix with dimension  $N(M+1)$ .  $\mathbf{D}$  is the  $N(M+1)$  diagonal matrix

$$\mathbf{D} = \text{diag}\{-C_1, \dots, -C_N, A - C_1, A - C_2, \dots, MA - C_N\} \quad (6)$$

Assuming that the wireless link will not change significantly during a small time interval, the link state evolves according to a birth-death Markov process, i.e.,  $\mu_{i,j} = 0$  for  $|i-j| > 1$ . Similar to the approach in [7], we couple the source producing process and the link service time variation process by (4) to obtain the equilibrium distribution of the queue occupancy. However, different from [7] which used an "on/off" two-state wireless channel model, we use a finite state wireless model with variable data rates which yields a more accurate representation of the channel state. Therefore, our results are more general.

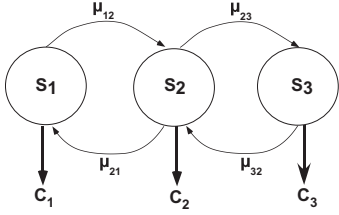


Fig. 2. Three state wireless channel model.

### C. Multiple hop wireless channel

To deliver video traffic from a home gateway to anywhere inside or even outside the home via power constrained wireless technologies with a limited transmission range (e.g., UWB), it is necessary to use multi-hop wireless relays. In this section, the fluid model is further extended to model the multi-hop wireless transmission scenario.

Assume that the indoor multi-hop wireless transmission consists of  $k$  hops. They are assumed to be within the interference range of each other, so they cannot transmit simultaneously, which is reasonable for a home networking environment. Since different hops require separate channel times in IEEE 802.15.3 CTAPs, the transmission rate of a packet from one end to the other end of the  $k$ -hop link is obtained as

$$r = \left[ \sum_{i=1}^k 1/r_i \right]^{-1}, \quad (7)$$

where  $r_i$  is the link data rate of the  $i$ -th hop.

The output of the previous hop can be seen as the input of the next hop, so multi-hop transmission can be viewed as a single virtual “link” which has an average data rate calculated by (7). The data rate variation of the virtual “link” depends on those of the wireless hops. Using  $k = 3$  as an example, according to (5), the generating matrix of the aggregated system is

$$\mathbf{B}_c = \mathbf{B}_{c1} \otimes \mathbf{I}_{N^2} + \mathbf{I}_N \otimes (\mathbf{B}_{c2} \otimes \mathbf{I}_N + \mathbf{I}_N \otimes \mathbf{B}_{c3}) \quad (8)$$

where  $\mathbf{B}_{c1}$ ,  $\mathbf{B}_{c2}$  and  $\mathbf{B}_{c3}$  are the generating matrices for the underlying continuous time Markov chains of the first, second and third hops, respectively.

The generating matrices of the three wireless hops are assumed to be i.i.d., with  $\mathbf{B}_{c1} = \mathbf{B}_{c2} = \mathbf{B}_{c3}$ . If each hop has three states corresponding to three different data rates, each matrix,  $\mathbf{B}_{c1}$  for instance, is a  $3 \times 3$  matrix with components represented by  $\mu_{ij}$ ,  $1 \leq i \leq 3$  and  $1 \leq j \leq 3$ .

The number of states for the aggregated system is  $N^3$ , where  $N$  is the number of states for each hop. With  $N = 3$ , the generating matrix for the multi-hop channel  $\mathbf{B}_c$  has dimension 27. We define the state of the multi-hop channel as

$$(1, 1, 1), (1, 1, 2), (1, 1, 3), (1, 2, 1), \dots, (3, 3, 3).$$

Thus, the index of the underlying Markov chain for the aggregated system is  $i = N^2(j_1 - 1) + N(j_2 - 1) + j_3$ ,  $1 \leq j_1, j_2, j_3 \leq 3$ ,  $1 \leq i \leq 27$ , where  $j_1$ ,  $j_2$  and  $j_3$  represent the states of the individual hops. The data rate of the multi-hop channel in state  $i$  can be calculated using (7).

Finally, substituting (8) and (7) into (5), (6) and (4), and using (2), we obtain the probability of buffer overflow in the multi-hop case, given by  $G(x)$ . Thus, given the QoS requirements of IPTV traffic, the admission region and buffer size can be derived.

## IV. PERFORMANCE EVALUATION BY SIMULATION

### A. Simulation setting

To verify the analytical results, extensive simulations have been performed using the Network Simulator NS-2 [9]. The H.264 video trace of “From Mars to China” in HDTV format (1920 x 1080i) is used [1]. The mean bit rate of the video source is 4.85 Mbps, the variance is  $3.6375 \times 10^{10}$  (bps)<sup>2</sup>, the auto-correlation decay coefficient is 0.215 bps, and the frame rate is 30 frames/sec. The video traffic is encapsulated in 1000 byte UDP packets. All routers use the simple drop-tail queue management scheme. The start times of any two video sources are offset by at least 5 seconds to reduce the correlation of the sources. We repeat the simulations with different random seeds and each simulation runs for 28 minutes. The simulation results presented are the averages of five runs.

The following parameters are used in our simulation unless otherwise explicitly stated. The link bandwidth of the wired backbone is 85 Mbps. The buffer size varies from 300 to 1000 packets. When simulating the IEEE 802.15.3 wireless network, the data rate of each wireless link follows a three state continuous time Markov chain, as shown in Fig. 2. The payload data rate is obtained by considering the physical layer data rate and the upper layer overheads. The data rate of the three states,  $R_i$ , are 55 Mbps, 110 Mbps, and 200 Mbps, respectively. The time to transmit a frame,  $T_{frame}$ , is

$$T_{frame} = T_a + \left( \frac{\text{payload} + RUI_h}{R_i} \right) + \left( \frac{PHY_h + MAC_h + HCS + FCS}{R_0} \right)$$

where  $T_a$ ,  $RUI_h$ ,  $PHY_h$ ,  $MAC_h$ ,  $HCS$  and  $FCS$  are the preamble time, RTP/UDP/IP headers, PHY header, MAC header, Header Check Sequence and Frame Check Sequence, respectively. The PHY/MAC overheads are transmitted at data rate  $R_0 = 28$  Mbps, and  $T_a$  is set to  $5 \mu s$ .

The achievable link-layer throughput is then given as

$$C_i = \frac{\text{payload} + RUI_h}{T_{frame} + T_g + T_{ACK} + 2SIFS}$$

where the guard time  $T_g$ , the ACK time  $T_{ACK}$ , the SIFS time and all other overheads take the same values as in [8]. This leads us to use rates  $C_1 = 40$  Mbps,  $C_2 = 64$  Mbps and  $C_3 = 88$  Mbps in states  $s_1$ ,  $s_2$  and  $s_3$ , respectively.

The state transition rates (1/sec) of the wireless link are given in the matrix  $\mathbf{B}_c$  below, where  $\mu_{ij}$  of the  $i^{th}$  row and the  $j^{th}$  column is the transition rate from state  $i$  to state  $j$ . Thus, the average link-layer data rate is about 85 Mbps.

$$\mathbf{B}_c = \begin{bmatrix} -18 & 18 & 0 \\ 2 & -16 & 14 \\ 0 & 2 & -2 \end{bmatrix}$$

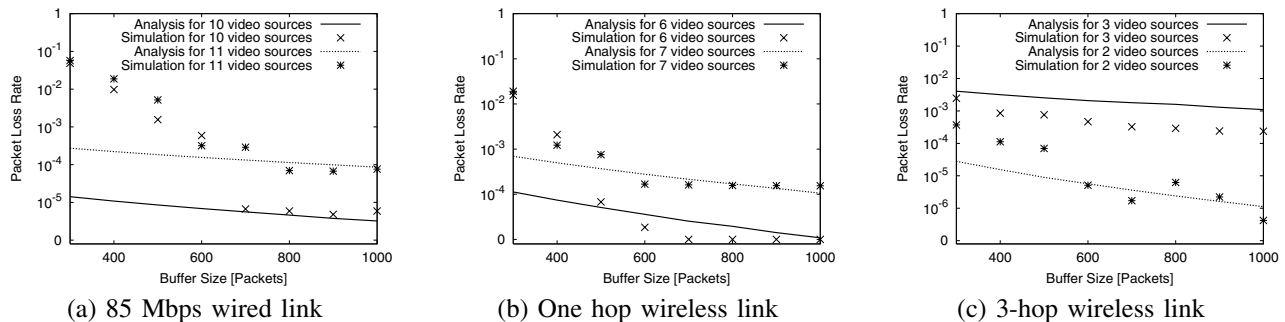


Fig. 3. Packet loss rate vs. buffer size.

## B. Numerical and simulation results

1) *Wired backbone network*: Fig. 3(a) shows the packet loss rate (PLR) vs. buffer size, with a link data rate of 85 Mbps. As the buffer size increases, the PLR decreases quickly when the buffer is less than 600 packets and then flattens out when the buffer size exceeds 700 packets. There are noticeable discrepancies between the simulation and analytical results when the buffer size is small, which can be explained as follows. The I and P frames of the video source can be more than 300 kilobytes, and a buffer size of more than 300 packets is needed to accommodate a single frame. The fluid model assumes that packets arrive at a CBR rate during the “on” state, so it cannot capture the burstiness within one frame. Thus, the analytical results are overly optimistic when the buffer size is small, and become accurate when the buffer size is larger. Since IPTV traffic can tolerate about 100 ms delay jitter, we can set the buffer size to be above 600 packets. In this region, the results using the fluid model are close to the simulation ones, and we can use the fluid model to determine the admission region of IPTV traffic accurately. In Fig. 3(a), both the analytical and simulation results show that, to ensure a loss rate less than  $10^{-4}$ , the admission region is 10 video sources with a buffer size no less than 700 packets.

2) *Wireless network*: For a one hop wireless link with an average data rate of 85 Mbps, as shown in Fig. 3(b), with a buffer size greater than 600 packets, the PLR drops below  $10^{-4}$  when admitting 6 video sources. The case when 7 video sources are admitted is also plotted on the same figure. In this case, the PLR is always greater than  $10^{-4}$ , even when the buffer size is greater than 600 packets. Thus, the maximum number of video sources that can be supported for the single hop wireless case is only 6. Comparing these results with those for the 85 Mbps wired link, the time-varying wireless link can admit far fewer video sources. This demonstrates that if we simply use the average data rate of a time-varying link to calculate the admission region, the results will be too optimistic.

The results for a three-hop wireless relay path are given in Fig. 3(c). The average data rate of each hop is still 85 Mbps. To maintain a PLR of  $10^{-4}$ , the maximum number of video sources is now only 2. As anticipated, an increase in the number of hops greatly affects the admission region. In fact,

the admission region for the three-hop wireless network is one-third that of the one-hop wireless case and one-fifth that of the 85 Mbps wired link.

## V. CONCLUSIONS

In this paper, we have investigated the IPTV packet-loss performance due to buffer overflow over wired and multi-hop wireless links. In addition, we have quantified the admission region for IPTV connections in a wireless and wired home network, given the link data rate, video traffic statistics, and QoS requirements. In a hybrid network consisting of both wired and wireless links, the admission region is determined by the one with the smallest capacity. The results obtained can help in planning future home networks. The admission regions in the presence of heterogeneous traffic will be an interesting further research issue.

## ACKNOWLEDGMENT

This work has been supported in part by a research grant from Bell University Laboratories (BUL) under the sponsorship of Bell Canada and an NSERC CRD grant.

## REFERENCES

- [1] P. Seeling and M. Reisslein, “Evaluating multimedia networking mechanisms using video traces,” *IEEE Potentials*, vol. 24, no. 4, pp. 21–25, Oct./Nov. 2005.
- [2] E. Shihab and L. Cai, “IPTV distribution technologies in broadband home networks,” *Proc. IEEE CCECE*, Vancouver, BC, Canada, Apr. 2007.
- [3] B. Maglaris, D. Anastassiou, P. Sen, G. Karlsson and J. Robbins, “Performance models of statistical multiplexing in packet video communications,” *IEEE Trans. Commun.*, vol. 36, no. 7, pp. 834–844, July 1988.
- [4] D. Anick, D. Mitra and M. M. Sondhi, “Stochastic theory of a data handling system with multiple sources,” *Bell Sys. Tech. J.*, vol. 61, pp. 1871–1894, Oct. 1982.
- [5] D. Mitra, “Stochastic theory of a fluid model of producers and consumers coupled by a buffer,” *Advances in Applied Probability*, vol. 20, no. 3, pp. 646–676, Sept. 1988.
- [6] A. J. Laub, *Matrix Analysis for Scientists and Engineers*, SIAM Publications, Philadelphia, PA, 2005.
- [7] J. Kim and M. Krunz, “Bandwidth allocation in wireless networks with guaranteed packet-loss performance,” *IEEE Trans. Networking*, vol. 8, no. 3, pp. 337–349, June 2000.
- [8] L. X. Cai, L. Cai, X. Shen and J. Mark, “Capacity of UWB networks supporting multimedia services,” *Proc. QShine*, Waterloo, ON, Canada, Aug. 2006.
- [9] The Network Simulator - NS-2, <http://www.isi.edu/nsnam/ns>.